



Continuous approximate synthesis of planar function-generators minimising the design error



Alexis Guigue^a, M. John D. Hayes^{b,*}

^aSoftree Technical Systems Inc., Vancouver, British Columbia, Canada

^bMechanical and Aerospace Engineering, Carleton University, Ottawa, Ontario, Canada

ARTICLE INFO

Article history:

Received 3 December 2015

Received in revised form 17 March 2016

Accepted 18 March 2016

Available online 6 April 2016

Keywords:

Approximate and continuous kinematic synthesis
Design error
Structural error
Function-generating linkage

ABSTRACT

It has been observed in the literature that as the cardinality of the prescribed discrete input–output data set increases, the corresponding four-bar linkages that minimise the Euclidean norm of the design and structural errors tend to converge to the same linkage. The important implication is that minimising the Euclidean norm, or any p -norm, of the structural error, which leads to a nonlinear least-squares problem requiring iterative solutions, can be accomplished implicitly by minimising that of the design error, which leads to a linear least-squares problem that can be solved directly. Apropos, the goal of this paper is to take the first step towards proving that as the cardinality of the data set tends towards infinity the observation is indeed true. In this paper we will integrate the synthesis equations in the range between minimum and maximum input values, thereby reposing the discrete approximate synthesis problem as a continuous one. Moreover, we will prove that a lower bound of the Euclidean norm, and indeed of any p -norm, of the design error for planar RRRR function-generating linkages exists and is attained with continuous approximate synthesis.

© 2016 Elsevier Ltd. All rights reserved.

1. Introduction

Design and structural errors are important performance indicators in the assessment and optimisation of function-generating linkages arising by means of approximate synthesis. The *design error* indicates the error residual incurred by a specific linkage in satisfying its synthesis equations. The *structural error*, in turn, is the difference between the prescribed linkage output value and the actual generated output value for a given input value [1]. From a design point of view it may be successfully argued that the structural error is the one that really matters, for it is directly related to the performance of the linkage.

It was shown in Ref. [2] that as the cardinality of the prescribed discrete input–output (I/O) data-set increases, the corresponding linkages that minimise the Euclidean norms of the design and structural errors tend to converge to the same linkage. The important implication of this observation is that the minimisation of the Euclidean norm of the structural error can be accomplished indirectly via the minimisation of the corresponding norm of the design error, provided that a suitably large number of I/O pairs is prescribed. The importance arises from the fact that the minimisation of the Euclidean norm of the design error leads to a linear least-squares problem whose solution can be obtained directly as opposed to iteratively [3,4], while the minimisation of the same norm of the structural error leads to a nonlinear least-squares problem, and hence, calls for an iterative solution [1].

* Corresponding author.

E-mail address: John.Hayes@carleton.ca (M. Hayes).

Several issues have arisen in the design error minimisation of four-bar linkages. First, the condition number of the synthesis matrix may lead to design parameters that poorly approximate the prescribed function [5]. This problem can be addressed through careful selection of the I/O pairs used to generate the synthesis matrix. It has also been suggested to introduce dial zeros whose values are chosen to minimise the condition number of the synthesis matrix [6]. Second, the identified design parameters have a dependence on the I/O set cardinality. As the number of I/O pairs grows, the magnitude of the design error tends to converge to a lower bound. Hence, the I/O set cardinality might be fixed as soon as the magnitude of the design error reaches some pre-defined minimum value [2].

Diverse interesting and useful optimisation strategies have been proposed recently for structural error minimisation in planar four-bar function-generators. For example, in Ref. [7] the authors define the least squares error between the desired and generated functions as the objective function for a sequential quadratic programming (SQP) approach. The proposed method solves a sequence of optimisation subproblems, each of which optimises a quadratic model of the objective function subject to a linearisation of the constraints based on the distribution of a finite set of precision points. Another novel approach which considers the minimisation of the structural error of the link lengths is described in Ref. [8]. The method treats one of the dyads as having fixed distances between joint centres, while the other dyad has links of variable length. The adjustable link lengths are varied using a discrete set of precision points as benchmarks. A completely different approach is used in Ref. [9] to develop a probabilistic, time-dependent function-generator synthesis method. The authors introduce the concept of “interval reliability synthesis”. The dimensions of the link lengths are treated as random variables while their mean values become the design variables, and the probability of failure to produce the function within a prescribed tolerance is minimised over a defined time interval and corresponding position level interval of the function. While these methods achieve excellent results, they do not shed any light on the curious tendency observed in Ref. [2]. What the vast body of literature reporting investigations into function-generator synthesis optimisation is missing is a systematic study of what the implications are of allowing the cardinal number of the I/O data set to tend towards infinity.

Hence, the goal of this paper is to take the first step towards proving that the convergence observed in Ref. [2] is true for planar four-bar function-generators. More precisely, a proof will be given for the design error that as the cardinality of the I/O data set increases from discrete numbers of I/O pairs to an infinite number between minimum and maximum pairs that a lower bound for any p -norm of the design error exists, and corresponds to that of the infinite I/O set, thereby changing the discrete approximate synthesis problem to a continuous approximate synthesis problem. To this end, the design error minimisation occurs in the space of a continuous function possessing an L_p norm defined later in this paper. However, our study is currently restricted to the planar RRRR function-generating linkage, where R denotes *revolute joint*, synthesised using the kinematic model defined in Ref. [10].

2. Design error minimisation: the discrete approximate approach

The synthesis problem of planar four-bar function-generators consists of determining all relevant design parameters such that the mechanism can produce a prescribed finite set of m I/O pairs, $\{\psi_i, \varphi_i\}_1^m$, where ψ_i and φ_i represent the i^{th} input and output variables, respectively, and m is the cardinality of the finite data-set. We define n to be the number of independent design parameters required to fully characterise the mechanism. For planar RRRR linkages, $n = 3$ [10]. If $m = n$, the problem is termed *exact synthesis* and may be considered a special case of approximate synthesis where $m > n$.

We consider the optimisation problem of planar four-bar function-generators as the approximate solution of an over-determined linear system of equations with the least error. The synthesis equations that are used to establish the linear system for a four-bar function-generator are the *Freudenstein equations* [10]. Consider the mechanism in Fig. 1. The i^{th} configuration is governed by:

$$k_1 + k_2 \cos(\varphi_i) - k_3 \cos(\psi_i) = \cos(\psi_i - \varphi_i), \tag{1}$$

where the k 's are the *Freudenstein parameters*, which are the following link length ratios:

$$k_1 = \frac{(a_1^2 + a_2^2 + a_4^2 - a_3^2)}{2a_2a_4}; \quad k_2 = \frac{a_1}{a_2}; \quad k_3 = \frac{a_1}{a_4}. \tag{2}$$

Given a set of three Freudenstein parameters, the corresponding set of link lengths, scaled by a_1 , are:

$$a_1 = 1; \quad a_2 = \frac{1}{k_2}; \quad a_4 = \frac{1}{k_3}; \quad a_3 = (1 + a_2^2 + a_4^2 - 2a_2a_4k_1)^{1/2}. \tag{3}$$

The finite set of I/O equations can be written in the following form, using Eq. (1)

$$\mathbf{Sk} = \mathbf{b}, \tag{4}$$

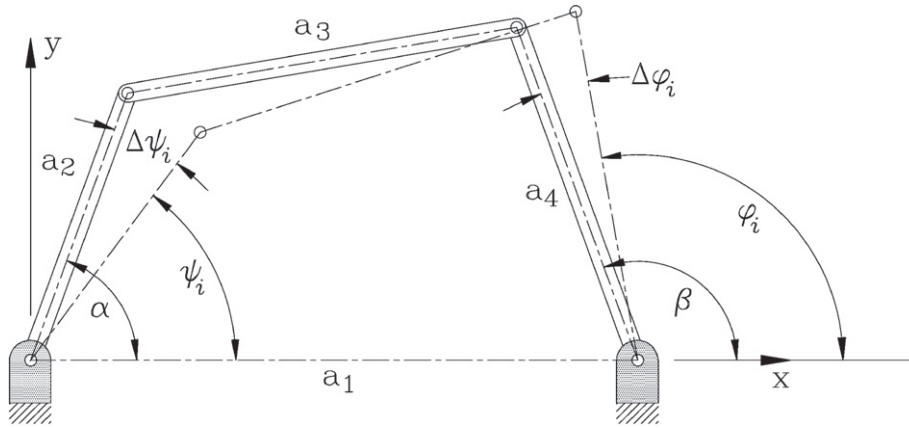


Fig. 1. A four-bar linkage in two configurations.

where \mathbf{S} is the $m \times 3$ synthesis matrix, whose i^{th} row is the 1×3 array \mathbf{s}_i , \mathbf{b} is an m -dimensional vector, whereas \mathbf{k} is the 3-dimensional vector of design variables called the Freudenstein parameters [10]. For the planar RRRR mechanism we have:

$$\mathbf{s}_i = [1 \cos \varphi_i - \cos \psi_i], \quad i = 1, \dots, m, \quad (5)$$

$$b_i = \cos(\psi_i - \varphi_i), \quad i = 1, \dots, m, \quad (6)$$

$$\mathbf{k} = [k_1 k_2 k_3]^T. \quad (7)$$

The synthesised linkage will only be capable of generating the desired function approximately. The design error is the algebraic difference of the left-hand side of Eq. (4) less the right-hand side. Because we will be comparing errors associated with different cardinalities, we now include the cardinality m in the definition. The m -dimensional design error vector \mathbf{d}_m for a finite discrete set of $m > 3$ I/O pairs, $\{(\psi_i, \varphi_i)_{i=1 \dots m}\}$, is defined as:

$$\mathbf{d}_m = \mathbf{S}_m \mathbf{k} - \mathbf{b}_m. \quad (8)$$

If the output values prescribed by the functional relationship, $\varphi_{pres,i}$, correspond precisely to the output values generated by the mechanism, i.e., $\varphi_{gen,i}$, then, $\|\mathbf{d}_m\| = 0$. However, for a general prescribed function $\varphi_{pres}(\psi)$, $\|\mathbf{d}_m\| \neq 0$ and we seek the Freudenstein parameter vector that minimises the norm of the design error vector. In general, the weighted Euclidian norm is used:

$$\|\mathbf{d}_m\|_{\mathbf{W}_m, 2}^2 = \frac{1}{2} \mathbf{d}_m^T \mathbf{W}_m \mathbf{d}_m, \quad (9)$$

where \mathbf{W}_m is an $m \times m$ diagonal matrix with strictly positive elements. In a typical design problem, \mathbf{W}_m is used to adjust the impact on the optimisation of specific I/O pairs. However, for the purposes of this work, \mathbf{W}_m will be set to the identity matrix, \mathbf{I}_m . The optimal Freudenstein parameters \mathbf{k}_m^* for this norm are:

$$\mathbf{k}_m^* = \mathbf{S}_m^+ \mathbf{b}_m, \quad (10)$$

where \mathbf{S}_m^+ is the Moore–Penrose generalised inverse of the synthesis matrix, and the corresponding minimal design error is:

$$\rightarrow \min_{\mathbf{k}} \|\mathbf{d}_m\|_2 = \|\mathbf{d}_m^*\|_2 = \|(\mathbf{I}_m - \mathbf{S}_m \mathbf{S}_m^+) \mathbf{b}_m\|_2. \quad (11)$$

In general, for any matrix, square or rectangular, the condition number κ is a measure of how invertible the matrix is: it is the ratio of the largest to smallest singular values. Consider the system of linear equations represented by $\mathbf{A}\mathbf{x} = \mathbf{b}$. The matrix \mathbf{A} may be viewed as a map from vector space \mathbf{x} to vector space \mathbf{b} . A very large condition number of \mathbf{A} implies that the smallest singular value of the matrix is very small, meaning that \mathbf{b} is poorly approximated by $\mathbf{A}\mathbf{x}$. This also implies that $\mathbf{A}^{-1}\mathbf{b}$ very poorly approximates \mathbf{x} . Extremely large condition numbers indicate that there is a near linear dependency among some of the rows of \mathbf{A} , meaning that one, or more, of its singular values is very close to zero. Such matrices are termed ill-conditioned. The

condition number κ is a property of the matrix \mathbf{A} and entirely independent of the vector spaces \mathbf{x} and \mathbf{b} . For numerical stability considerations, it is always desirable to have a well-conditioned synthesis matrix, otherwise the numerical values of \mathbf{S}_m^+ may be significantly distorted by very small singular values, or singular values identically equal to zero, leading to optimised \mathbf{k} that imply a mechanism which very poorly approximates the function. Hence, the dial zeros α and β , illustrated in Fig. 1, have been introduced to minimise the condition number, κ , of \mathbf{S}_m :

$$\psi_i = \alpha + \Delta\psi_i; \quad \varphi_i = \beta + \Delta\varphi_i. \tag{12}$$

When the dial zeros are substituted into Eq. (1), the synthesis equation becomes:

$$k_1 + k_2 \cos(\beta + \Delta\varphi_i) - k_3 \cos(\alpha + \Delta\psi_i) = \cos(\alpha + \Delta\psi_i - \beta - \Delta\varphi_i), \tag{13}$$

and, the I/O pairs are regarded as a discrete set of incremental angular changes $\{(\Delta\psi_i, \Delta\varphi_i)_{i=0..m}\}$. The arrays \mathbf{d}_m^* , \mathbf{k}_m^* and \mathbf{S}_m are now also functions of the dial zeros. With this modification, the design error minimisation problem can be efficiently solved in a least squares sense in two steps:

1. determine the dial zeros to minimise the condition number $\kappa_m(\alpha, \beta)$ of the synthesis matrix \mathbf{S}_m ;
2. determine the corresponding optimal Freudenstein parameters using Eq. (10).

3. Design error minimisation: the continuous approximate approach

A major issue associated with the discrete approach to the design error minimisation is the appropriate choice for the cardinality of the discrete I/O pair data set such that the minimisation of the structural error is implied. Indeed, the choice of m depends on the prescribed function $\Delta\varphi_{pres}(\Delta\psi)$ and m is generally fixed when some level of convergence is observed. For the example used in Ref. [2] $m = 40$ was observed to be a good choice. We now propose to evaluate the design error over the continuous range between minimum and maximum, or initial and final, input values of the prescribed function, denoted $[\Delta\psi_0, \Delta\psi_f]$. We only consider functions that are continuous over $[\Delta\psi_0, \Delta\psi_f]$, that are defined in a function space, denoted $C^0([\Delta\psi_0, \Delta\psi_f])$, whereupon the following L_p -norm has been defined for any continuous function f on the closed interval $[\Delta\psi_0, \Delta\psi_f]$:

$$\forall f \in C^0([\Delta\psi_0, \Delta\psi_f]), \|f\|_p = \left(\int_{\Delta\psi_0}^{\Delta\psi_f} |f(\psi)|^p d\psi \right)^{1/p}, \tag{14}$$

where p is an integer such that $p \geq 1$. Imposing the L_p -norm upon this function space makes $C^0([\Delta\psi_0, \Delta\psi_f])$ an L_p -space. Such L_p -spaces are defined using a generalisation of the vector norm for finite-dimensional vector spaces [4]. Vector norms are special cases of the family of L_p -norms, often denoted by l_p while L_p is reserved for norms in function spaces [4]. The most common L_p -norms for a continuous function f on a closed interval $[a, b]$, and in fact, the most commonly used vector norms [11], are the maximum or Chebyshev norm, the Euclidean norm, and the so called Manhattan norm¹ which are respectively defined by:

$$\|f\|_\infty = \max_{x \in [a,b]} |f(x)|; \tag{15}$$

$$\|f\|_2 = \left(\int_a^b f(x)^2 dx \right)^{1/2}; \tag{16}$$

$$\|f\|_1 = \int_a^b |f(x)| dx. \tag{17}$$

The Manhattan and Chebyshev norms are the limiting cases ($p = 1$ and $p = \infty$, respectively) of the family of L_p -norms [4]. The L_p -norms obey the following relationship:

$$\|f\|_\infty \leq \dots \leq \|f\|_2 \leq \|f\|_1. \tag{18}$$

Typically, the most appropriate norm must be selected to evaluate the magnitude of the objective function for the error minimisation, given a function that is to be approximated by the resulting linkage. However, it turns out that Lawson's

¹ The term Manhattan norm arises because the vector norm corresponds to sums of distances along the basis vector directions, as one would travel along a rectangular street plan.

algorithm [12,13] can be used to sequentially minimise the Chebyshev norm via the minimisation of the Euclidean norm [14]. This means that the continuous approximate approach to the design error minimisation is independent of the L_p -norm because it applies to both the Chebyshev and Euclidean norms, and hence all intermediate ones. Therefore, without loss in generality the Euclidean norm will be used in the example in Section 5, which follows the development of the approach.

Assuming that the prescribed function belongs to $C^0([\Delta\psi_0, \Delta\psi_f])$, the design error is defined using the Euclidean norm, though any L_p -norm could be used [14]:

$$\|\mathbf{d}(\alpha, \beta)\|_2 = \left(\int_{\Delta\psi_0}^{\Delta\psi_f} (k_1 + k_2 \cos(\beta + \Delta\varphi) - k_3 \cos(\alpha + \Delta\psi) - \cos(\alpha + \Delta\psi - \beta - \Delta\varphi))^2 d\Delta\psi \right)^{\frac{1}{2}}. \quad (19)$$

After some algebraic manipulation, it can be shown that the square of Eq. (19) is a quadratic function in terms of the Freudenstein parameters:

$$\|\mathbf{d}(\alpha, \beta)\|_2^2 = \mathbf{k}^T \mathbf{A}(\alpha, \beta) \mathbf{k} - 2\mathbf{e}(\alpha, \beta)^T \mathbf{k} + c(\alpha, \beta). \quad (20)$$

The matrix $\mathbf{A}(\alpha, \beta)$ is a 3×3 symmetric positive semidefinite matrix whose six distinct elements a_{ij} are:

$$\begin{aligned} a_{11} &= \int_{\Delta\psi_0}^{\Delta\psi_f} d\Delta\psi = \Delta\psi_f - \Delta\psi_0; \\ a_{12} &= \int_{\Delta\psi_0}^{\Delta\psi_f} \cos(\beta + \Delta\varphi) d\Delta\psi; \\ a_{13} &= - \int_{\Delta\psi_0}^{\Delta\psi_f} \cos(\alpha + \Delta\psi) d\Delta\psi; \\ a_{22} &= \int_{\Delta\psi_0}^{\Delta\psi_f} \cos^2(\beta + \Delta\varphi) d\Delta\psi; \\ a_{23} &= - \int_{\Delta\psi_0}^{\Delta\psi_f} \cos(\beta + \Delta\varphi) \cos(\alpha + \Delta\psi) d\Delta\psi; \\ a_{33} &= \int_{\Delta\psi_0}^{\Delta\psi_f} \cos^2(\alpha + \Delta\psi) d\Delta\psi; \end{aligned}$$

while $\mathbf{e}(\alpha, \beta)$ is a 3-dimensional vector whose elements are:

$$\begin{aligned} e_1 &= \int_{\Delta\psi_0}^{\Delta\psi_f} \cos(\alpha + \Delta\psi - \beta - \Delta\varphi) d\Delta\psi; \\ e_2 &= \int_{\Delta\psi_0}^{\Delta\psi_f} (\cos(\beta + \Delta\varphi) \cos(\alpha + \Delta\psi - \beta - \Delta\varphi)) d\Delta\psi; \\ e_3 &= - \int_{\Delta\psi_0}^{\Delta\psi_f} (\cos(\alpha + \Delta\psi) \cos(\alpha + \Delta\psi - \beta - \Delta\varphi)) d\Delta\psi; \end{aligned}$$

and finally $c(\alpha, \beta)$ is a scalar having the form:

$$c = \int_{\Delta\psi_0}^{\Delta\psi_f} \cos^2(\alpha + \Delta\psi - \beta - \Delta\varphi) d\Delta\psi.$$

When $\mathbf{A}(\alpha, \beta)$ is positive definite, the optimal Freudenstein parameters $\mathbf{k}^*(\alpha, \beta)$ which minimise $\|\mathbf{d}(\alpha, \beta)\|_2^2$ (or equivalently $\|\mathbf{d}(\alpha, \beta)\|_2$) are:

$$\mathbf{k}^*(\alpha, \beta) = \mathbf{A}^{-1}(\alpha, \beta) \mathbf{e}(\alpha, \beta), \quad (21)$$

and the square of the minimal design error is:

$$\min_{\mathbf{k}} \|\mathbf{d}(\alpha, \beta)\|_2^2 = \|\mathbf{d}^*(\alpha, \beta)\|_2^2 = c(\alpha, \beta) - \mathbf{e}(\alpha, \beta)^T \mathbf{A}^{-1}(\alpha, \beta) \mathbf{e}(\alpha, \beta). \quad (22)$$

The assumption of positive definiteness for $\mathbf{A}(\alpha, \beta)$ will be discussed in Section 4. However, a necessary condition for $\mathbf{A}(\alpha, \beta)$ to be positive definite is that it is non-singular. This justifies *a posteriori* why we use the dial zeros. In this case, as in Section 2, the design error minimisation problem is solved in two steps:

1. determine the dial zeros to minimise the condition number $\kappa(\alpha, \beta)$ of $\mathbf{A}(\alpha, \beta)$;
2. determine the corresponding optimal Freudenstein parameters using Eq. (21).

Intuitively, the continuous approximate approach should correspond to the limit of the discrete approximate approach. This is proven to be so in the next section.

4. The design error of the discrete approximate approach is lower bounded by that of the continuous approximate approach

In this section, we assume that $\Delta\varphi_{pres}(\Delta\psi)$ is a continuously differentiable function, however Propositions 1, 2, and 3, which follow, only require continuity. With this assumption and using the notation introduced in the previous sections, the following propositions hold.

Proposition 1. $\mathbf{A}(\alpha, \beta)$ is positive semidefinite, and

$$\lim_{m \rightarrow \infty} \kappa_m(\alpha, \beta) = \kappa(\alpha, \beta).$$

Proposition 2. If $\mathbf{A}(\alpha, \beta)$ possesses full rank, then,

$$\lim_{m \rightarrow \infty} \mathbf{k}_m^*(\alpha, \beta) = \mathbf{k}^*(\alpha, \beta).$$

Recall that $\mathbf{k}^*(\alpha, \beta)$ minimises the design error under the condition that $\mathbf{A}(\alpha, \beta)$ is positive definite. Now, from Proposition 1, we can claim that $\mathbf{A}(\alpha, \beta)$ is at least positive semidefinite. However, the positive definiteness is not guaranteed and it justifies the need for the assumption in Proposition 2.

Proposition 3. If $\mathbf{A}(\alpha, \beta)$ possesses full rank, then,

$$\lim_{m \rightarrow \infty} \frac{\Delta\psi_f - \Delta\psi_0}{m} \|\mathbf{d}_m^*(\alpha, \beta)\|_2 = \|\mathbf{d}^*(\alpha, \beta)\|_2.$$

Proposition 4. Let (α^*, β^*) be the dial zero pair that minimises $\kappa(\alpha, \beta)$. If the optimal solution (α^*, β^*) is unique, then,

$$\lim_{m \rightarrow \infty} (\alpha_m^*, \beta_m^*) = (\alpha^*, \beta^*).$$

Proposition 5. If the optimal solution (α^*, β^*) is unique, then,

$$\lim_{m \rightarrow \infty} \kappa_m(\alpha_m, \beta_m) = \kappa(\alpha^*, \beta^*).$$

Moreover, if $\mathbf{A}(\alpha^*, \beta^*)$ possesses full rank, then,

$$\lim_{m \rightarrow \infty} \mathbf{k}_m^*(\alpha_m, \beta_m) = \mathbf{k}^*(\alpha^*, \beta^*),$$

and

$$\lim_{m \rightarrow \infty} \frac{\Delta\psi_f - \Delta\psi_0}{m} \|\mathbf{d}_m^*(\alpha_m, \beta_m)\|_2 = \|\mathbf{d}^*(\alpha^*, \beta^*)\|_2.$$

Proposition 5 is our main result. It essentially states that the optimal Freudenstein parameters and the minimal design error for the discrete approach converge to the optimal Freudenstein parameters and the minimal design error for the continuous approach.

4.1. Proofs

Proof of Proposition 1. the proof of Proposition 1 requires the following result.

Proposition 6. Let f be a continuous function on some interval $[a, b]$, then [4]

$$\lim_{n \rightarrow +\infty} \sum_{i=0}^{n-1} \frac{b-a}{n} f\left(a + i \frac{b-a}{n}\right) = \int_a^b f(x) dx.$$

From Proposition 6, the elements of $\mathbf{A}_m(\alpha, \beta) = \frac{\Delta\psi_f - \Delta\psi_0}{m} \mathbf{S}_m^T(\alpha, \beta) \mathbf{S}_m(\alpha, \beta)$ converge to the elements of $\mathbf{A}(\alpha, \beta)$.

Recall the definitions for positive definiteness and positive semidefiniteness: a real $n \times n$ matrix \mathbf{A} is positive definite if, for all vectors $\mathbf{x} \in \mathbb{R}$, $\mathbf{x}^T \mathbf{A} \mathbf{x} > 0$, and positive semidefinite if, for all vectors $\mathbf{x} \in \mathbb{R}$, $\mathbf{x}^T \mathbf{A} \mathbf{x} \geq 0$. Now, from the definitions of the elements a_{ij} of $\mathbf{A}(\alpha, \beta)$ we have

$$\mathbf{A}(\alpha, \beta) = \int_{\Delta\psi_0}^{\Delta\psi_f} \mathbf{B} d\Delta\psi, \tag{23}$$

where \mathbf{B} is a symmetric 3×3 matrix:

$$\mathbf{B} = \begin{bmatrix} 1 & \cos(\beta + \Delta\varphi) & -\cos(\alpha + \Delta\psi) \\ \cos(\beta + \Delta\varphi) & \cos^2(\beta + \Delta\varphi) & -\cos(\beta + \Delta\varphi)\cos(\alpha + \Delta\psi) \\ -\cos(\alpha + \Delta\psi) & -\cos(\beta + \Delta\varphi)\cos(\alpha + \Delta\psi) & \cos^2(\alpha + \Delta\psi) \end{bmatrix}. \tag{24}$$

Matrix \mathbf{B} has the special property that it is the vector product of vector \mathbf{v} and its transpose, where

$$\mathbf{v} = \begin{bmatrix} 1 \\ \cos(\beta + \Delta\varphi) \\ -\cos(\alpha + \Delta\psi) \end{bmatrix}, \tag{25}$$

such that

$$\mathbf{v} \mathbf{v}^T = \mathbf{B}. \tag{26}$$

Then, for each vector $\mathbf{x} = [x_1, x_2, x_3]^T$ in \mathbb{R}^3 the function

$$f(\mathbf{x}, \Delta\psi) = \mathbf{x}^T \mathbf{B} \mathbf{x}$$

has only non-negative values, as

$$f(\mathbf{x}, \Delta\psi) = \mathbf{x}^T \mathbf{B} \mathbf{x} = \mathbf{x}^T (\mathbf{v} \mathbf{v}^T) \mathbf{x} = (\mathbf{x}^T \mathbf{v})^2 \geq 0.$$

From this result, it necessarily follows that

$$\mathbf{x}^T \mathbf{A} \mathbf{x} = \mathbf{x}^T \left(\int_{\Delta\psi_0}^{\Delta\psi_f} \mathbf{B} d\Delta\psi \right) \mathbf{x} = \int_{\Delta\psi_0}^{\Delta\psi_f} (\mathbf{x}^T \mathbf{B} \mathbf{x}) d\Delta\psi = \int_{\Delta\psi_0}^{\Delta\psi_f} f(\mathbf{x}, \Delta\psi) d\Delta\psi \geq 0,$$

which completes the proof. Now, given an arbitrary function, the function-generator designer need only check that the eigenvalues of the matrix \mathbf{A} defined by the given function are all greater than zero.

Proof of Proposition 2. the proof of Proposition 2 requires the following proposition.

Proposition 7. If a sequence of matrices \mathbf{M}_n converges to a matrix \mathbf{M} and \mathbf{M} is invertible then, \mathbf{M}_n^{-1} converges to \mathbf{M}^{-1} [15].

From Proposition 1, $\mathbf{A}_m(\alpha, \beta)$ converges towards $\mathbf{A}(\alpha, \beta)$. $\mathbf{A}(\alpha, \beta)$ possesses full rank by hypothesis, then there must be some index m_0 such that $\forall m \geq m_0$ and $\mathbf{A}_m(\alpha, \beta)$ possesses full rank. Hence, $\forall m \geq m_0$ $\mathbf{S}_m(\alpha, \beta)$ possesses full rank and the pseudo-inverse $\mathbf{S}_m^+(\alpha, \beta)$ is:

$$\mathbf{S}_m^+(\alpha, \beta) = (\mathbf{S}_m^T(\alpha, \beta) \mathbf{S}_m(\alpha, \beta))^{-1} \mathbf{S}_m^T(\alpha, \beta) = \frac{\Delta\psi_f - \Delta\psi_0}{m} \mathbf{A}_m^{-1}(\alpha, \beta) \mathbf{S}_m^T(\alpha, \beta). \tag{27}$$

Eq. (10) then becomes:

$$\mathbf{k}_m^*(\alpha, \beta) = \mathbf{A}_m^{-1}(\alpha, \beta) \left(\frac{\Delta\psi_f - \Delta\psi_0}{m} \mathbf{S}_m^T(\alpha, \beta) \mathbf{b}_m(\alpha, \beta) \right). \quad (28)$$

From Proposition 6, $\left(\frac{\Delta\psi_f - \Delta\psi_0}{m} \mathbf{S}_m^T(\alpha, \beta) \mathbf{b}_m(\alpha, \beta) \right)$ converges to $\mathbf{e}(\alpha, \beta)$. From Proposition 7, $\mathbf{A}_m^{-1}(\alpha, \beta)$ converges towards $\mathbf{A}^{-1}(\alpha, \beta)$, hence $\mathbf{k}_m^*(\alpha, \beta)$ converges towards $\mathbf{A}^{-1}(\alpha, \beta) \mathbf{e}(\alpha, \beta)$ which is equal to $\mathbf{k}^*(\alpha, \beta)$ in Eq. (21). This completes the proof.

Proof of Proposition 3. Eq. (11) can be rewritten:

$$\| \mathbf{d}_m^*(\alpha, \beta) \|_2^2 = \mathbf{b}_m^T(\alpha, \beta) \mathbf{b}_m(\alpha, \beta) - \left(\mathbf{S}_m^T(\alpha, \beta) \mathbf{b}_m(\alpha, \beta) \right)^T \mathbf{k}_m^*(\alpha, \beta). \quad (29)$$

Multiply Eq. (29) by $\frac{\Delta\psi_f - \Delta\psi_0}{m}$. From Proposition 6, $\left(\frac{\Delta\psi_f - \Delta\psi_0}{m} \mathbf{S}_m^T(\alpha, \beta) \mathbf{b}_m(\alpha, \beta) \right)$ converges to $\mathbf{e}(\alpha, \beta)$ and $\left(\frac{\Delta\psi_f - \Delta\psi_0}{m} \mathbf{b}_m^T(\alpha, \beta) \mathbf{b}_m(\alpha, \beta) \right)$ converges to $c(\alpha, \beta)$. From Proposition 2, $\mathbf{k}_m^*(\alpha, \beta)$ converges towards $\mathbf{k}^*(\alpha, \beta)$. This completes the proof.

Proof of Proposition 4. the proof of Proposition 4 requires the following proposition:

Proposition 8. Let f be a function continuously differentiable on $[a, b]$, then [16]

$$\left| \int_a^b f(x) dx - \lim_{n \rightarrow +\infty} \sum_{i=0}^{n-1} \frac{b-a}{n} f\left(a + i \frac{b-a}{n}\right) \right| \leq \frac{(b-a) \max\{f'(x), x \in [a, b]\}}{n}.$$

The dial zeros are members of a compact set defined by the Cartesian product $K = [-\pi, \pi] \times [-\pi, \pi]$. Hence, the maximum of the first derivative of any entry of $\mathbf{A}_m(\alpha, \beta)$ is bounded uniformly relative to (α, β) . From Proposition 8, it follows that the elements of $\mathbf{A}_m(\alpha, \beta)$ converge uniformly relative to (α, β) towards the elements of $\mathbf{A}(\alpha, \beta)$.

The sequence (α_m^*, β_m^*) belongs to K . Hence, there exists a subsequence $(\alpha_{\varphi(m)}^*, \beta_{\varphi(m)}^*)$ which converges to some $(\alpha_\varphi^*, \beta_\varphi^*)$. From the uniform convergence of $\mathbf{A}_m(\alpha, \beta)$, it follows that the elements of $\mathbf{A}_{\varphi(m)}(\alpha_{\varphi(m)}^*, \beta_{\varphi(m)}^*)$ converge towards the elements of $\mathbf{A}(\alpha_\varphi^*, \beta_\varphi^*)$. Following the same arguments used in the proof of Proposition 1, we get:

$$\lim_{m \rightarrow \infty} \kappa_{\varphi(m)}(\alpha_{\varphi(m)}^*, \beta_{\varphi(m)}^*) = \kappa(\alpha_\varphi^*, \beta_\varphi^*), \quad (30)$$

or $(\alpha_{\varphi(m)}^*, \beta_{\varphi(m)}^*)$ minimises the condition number of $\mathbf{A}_{\varphi(m)}(\alpha, \beta)$, hence:

$$\forall (\alpha, \beta) \in K, \kappa_{\varphi(m)}(\alpha_{\varphi(m)}^*, \beta_{\varphi(m)}^*) \leq \kappa_{\varphi(m)}(\alpha, \beta).$$

From Eq. (30) and Proposition 1, taking the limit on both sides of this inequality gives:

$$\forall (\alpha, \beta) \in K, \kappa(\alpha_\varphi^*, \beta_\varphi^*) \leq \kappa(\alpha, \beta).$$

Hence, $(\alpha_\varphi^*, \beta_\varphi^*)$ minimises the condition number of $\mathbf{A}(\alpha, \beta)$. In other words, each convergent (α_m^*, β_m^*) converges to a minimum of the condition number of $\mathbf{A}(\alpha, \beta)$. By hypothesis, this minimum is unique. Hence, $\forall \varphi, (\alpha_\varphi^*, \beta_\varphi^*) = (\alpha^*, \beta^*)$ and the whole sequence (α_m^*, β_m^*) converges to (α^*, β^*) . This completes the proof.

Proof of Proposition 5. the first statement of Proposition 5 has been proved in the proof of Proposition 4, see Eq. (30). From the uniform convergence arising from Proposition 8 the convergence in Proposition 2 and Proposition 3 is in fact uniform. The last two statements of Proposition 5 follow. To be completely rigorous, Proposition 7 should be modified to uniform convergence, but doing so introduces no contradictions.

5. Example

The preceding results for continuous approximate synthesis that minimises the design error are now illustrated with an example. Let the prescribed function be the Ackerman steering condition for terrestrial vehicles. The steering condition can be expressed as a trigonometric function whose variables are illustrated in Fig. 2:

$$\sin(\Delta\varphi_{pres} - \Delta\psi) - \rho \sin(\Delta\psi) \sin(\Delta\varphi_{pres}) = 0, \quad (31)$$

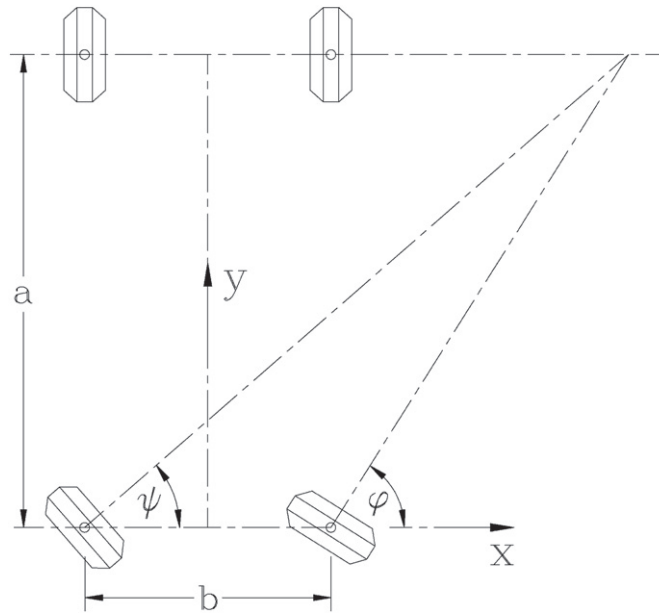


Fig. 2. Graphical illustration of the Ackerman steering condition.

with ρ denoting the length ratio b/a , where a is the distance between front and rear axles, and b the distance between the pivots of the wheel-carriers, which are coupled to the chassis. With the dial zeros, the expression for the steering condition becomes:

$$\sin(\beta + \Delta\varphi_{pres} - \alpha - \Delta\psi) - \rho \sin(\alpha + \Delta\psi) \sin(\beta + \Delta\varphi_{pres}) = 0. \tag{32}$$

For our example, $\rho = 0.5$ and $[\Delta\psi_0, \Delta\psi_f] = [-40.00, 30.00]$, where angles are specified in degrees. With these values, the prescribed function, i.e. the steering condition, is continuously differentiable. Hence, Proposition 5 must apply.

5.1. Establishing the optimal dial zeros and Freudenstein parameters

The multi-dimensional Nelder–Mead downhill simplex algorithm [17] is employed to find the optimal values for the dial zeros. Table 1 lists (α_m^*, β_m^*) for different values of m , as well as (α^*, β^*) . From the optimal dial zeros obtained in Table 1, it is now possible to compute the optimal Freudenstein parameters. Table 2 lists the optimised Freudenstein parameters, k_i , synthesis matrix condition numbers κ_m , and design error norms which have been normalised by \sqrt{m} for comparison for different values of m as well as the values using the continuous approach.

Continuous approximate synthesis eliminates the problem of determining an appropriate cardinal number for the data-set because it evaluates the case for $m \rightarrow \infty$. Hence there is no need to search for some convergence in order to set the proper value of m , which eliminates a source of error. However, the continuous approach requires numerical integrations, which itself is a source of error. These errors are in fact of the same nature. Indeed, from the development of Section 4, it is clear that discrete approximate synthesis is essentially a numerical integration method itself: Romberg’s method for example, which is an extrapolation on the trapezoidal rule [4]. Hence, comparing the errors arising from the discrete approximate synthesis with continuous approximate synthesis is equivalent to comparing the error terms of two different numerical integration methods. The example presented above employed the Matlab function *quadl*, which employs recursive adaptive Lobatto quadrature [18].

Table 1
Optimal dial zeros.

m	α_m^*	β_m^*	α^*	β^*
10	−61.80	67.320	−	−
40	−62.17	68.73	−	−
100	−62.23	69.03	−	−
400	−62.26	69.17	−	−
1000	−62.27	69.20	−	−
∞	−	−	−62.27	69.22

Table 2
Optimised Freudenstein parameters, condition numbers, and normalised design errors.

m	k_1	k_2	k_3	κ_m	κ^*	$\ \mathbf{d}_m\ _2$	$\ \mathbf{d}^*\ _2$
10	−0.993	0.412	−0.429	18.24	–	6.93×10^{-4}	–
40	−1.001	0.406	−0.425	20.79	–	6.44×10^{-4}	–
100	−1.003	0.405	−0.424	21.38	–	6.31×10^{-4}	–
400	−1.003	0.404	−0.424	21.69	–	6.24×10^{-4}	–
1000	−1.004	0.404	−0.424	21.75	–	6.23×10^{-4}	–
∞	−1.004	0.404	−0.424	–	475.03	–	6.23×10^{-4}

6. Conclusions and future work

In this paper a proof has been given that the design error of planar RRRR function-generating linkages synthesised using over-constrained systems of equations established with discrete I/O data sets is bounded by a minimum value established using continuous approximate synthesis between minimum and maximum I/O values. Evaluating the design error over the entire continuous range of the function requires the use of a functional normed space, thereby changing the discrete approximate synthesis problem to a continuous approximate synthesis problem. Assuming that the prescribed function $\Delta\varphi_{pres}(\Delta\psi)$ is continuously differentiable, it is shown that the dial zeros, the optimal Freudenstein parameters, and the minimal design error for discrete approximate synthesis converge towards the dial zeros, the optimal Freudenstein parameters and the minimal design error for continuous approximate synthesis. In other words, the continuous approach corresponds to the discrete approach after setting the cardinality of the I/O set to $m \rightarrow \infty$, and represents the bounding optimal values.

The extension of this work is to investigate how the structural error as defined in Ref. [2] bounds the design error. First, it should be determined whether the structural error minimisation problem can be formulated and, more importantly solved, using the continuous approach. Second, it should be investigated whether in this case too, the continuous approach corresponds to the discrete approach with $m \rightarrow \infty$. This is certainly much more challenging due to the increased complexity of the continuous structural error minimisation problem, which is a non-linear problem with equality constraints, compared to the continuous design error minimisation problem, which is a quadratic problem without any constraints. Finally, one might ask whether our developments could be applied to other mechanism topologies, such as planar mechanisms possessing prismatic joints, as well as spherical, or spatial linkages.

Acknowledgments

The authors gratefully acknowledge partial financial support for this work provided by a research grant from the *Natural Sciences and Engineering Research Council of Canada* (NSERC) (250012–2011).

References

- [1] S.O. Tinubu, K.C. Gupta, Optimal synthesis of function generators without the branch defect, *ASME, J. of Mech., Trans., and Autom. in Design* 106 (1984) 348–354.
- [2] M.J.D. Hayes, K. Parsa, J. Angeles, The effect of data-set cardinality on the design and structural errors of four-bar function-generators, *Proceedings of the Tenth World Congress on the Theory of Machines and Mechanisms*, Oulu, Finland, 1999, 437–442.
- [3] D.J. Wilde, Error synthesis in the least-squares design of function generating mechanisms, *ASME, J. of Mechanical Design* 104 (1982) 881–884.
- [4] G.B. Dahlquist, Å. Björck, *Numerical Methods*, translated by Anderson, Prentice-Hall, Inc., U.S.A. 1969.
- [5] Z. Liu, J. Angeles, Data conditioning in the optimization of function-generating linkages, *Advances in Design Automation: Proc. 19th Annual ASME Design Automation Conference*, 1993, 419–426.
- [6] Z. Liu, *Kinematic Optimization of Linkages*, Dept. of Mech. Eng., McGill University, Montréal, QC, Canada, 1993. (Ph.D. thesis)
- [7] M. Shariati, M. Norouzi, Optimal synthesis of function generator of four-bar linkages based on distribution of precision points, *Mechanica* 46 (5) (2011) 1007–1021.
- [8] C. Peng, R.S. Sohdi, Optimal synthesis of adjustable mechanisms generating multi-phase approximate paths, *Mech. Mach. Theory* 45 (7) (2010) 989–996.
- [9] J. Zhang, J. Wang, X. Du, Time-dependent probabilistic synthesis for function generator mechanisms, *Mech. Mach. Theory* 46 (9) (2011) 1236–1250.
- [10] F. Freudenstein, Approximate synthesis of four-bar linkages, *Trans. ASME* 77 (1955) 853–861.
- [11] J.E. Gentle, *Numerical Linear Algebra for Applications in Statistics*, Springer, New York, U.S.A. 1998.
- [12] C.L. Lawson, *Contributions to the Theory of Linear Least Maximum Approximations*, UCLA, Los Angeles, California, U.S.A., 1961. (Ph.D. thesis)
- [13] J.R. Rice, K.H. Usow, The Lawson algorithm and extensions, *Math. Comput.* 22 (101) (December 1967) 118–126.
- [14] F. Angeles, J. Angeles, Synthesis of function-generating linkages with minimax structural error: the linear case, *Proc. 13th IFTOMM World Congress*, June 2011.
- [15] J. Ercolano, Golden sequences of matrices with application to Fibonacci algebra, *The Fibonacci Quarterly* 15 (5) (December 1976) 419–426.
- [16] N.B. Haaser, J.A. Sullivan, *Real Analysis*, Van Nostrand Reinhold Co., New York, U.S.A. 1971.
- [17] J.A. Nelder, R. Mead, A simplex method for function minimization, *Computer Journal* 7 (4) (1965) 308–313.
- [18] L.F. Shampine, Vectorized adaptive quadrature in MATLAB, *J. Comput. Appl. Math.* 211 (February 2008) 131–140.